ÉCOLE POLYTECHNIQUE
FÉDÉRALE DE LAUSANNE

Semester Project

Engineering Mechanincs of Soft Interfaces (EMSI) - EPFL

FTIR Calibration

Project Report

January 12, 2019

Author:
Dylan Hade

Supervisor:
Prof. John Kolinski
Assistant:
Ramin Kaviani

Abstract

This report describes what was done during a Master's semester project lasting 14 weeks and concerns the calibration of Frustrated Total Internal Reflection (FTIR) and optimizing the setup for measuring the thin layer of air trapped between an impacting droplet and a solid surface before total wetting occurs. For this, a LED light source illuminating a prism is used, and a high speed camera reads the reflected image which can be analysed and can give the thickness of the layer or gap between the droplet and the solid surface, as the reflected light intensity read by the camera is directly a function of this gap thickness. To calibrate the setup a spherical lens is placed on top of the prism and its elastically deformed profile (under its own weight) is measured thanks to the FTIR setup, and compared to the analytical solution for the deformed profile provided by Hertzian solid contact theory. The measures are investigated with the light source being polarized and therefore the differences between the results of $s-$ and $p-$polarized light are directly compared. It is found that $s-$polarized light gives a higher quality image with less error and noise and therefore $s-$polarized light is used for the rest of the calibration. A new intensity normalization method is investigated and appears to yield very promising results with low error considering the nanometer scale of deformation. After completion of the calibration, a droplet impact was tested and the image revealed that a pulsing LED would yield better results given that the very high velocity at which the layer of air disappears as the liquid completely wets the solid surface requires a very high framerate.

Nomenclature

Exponents

i	Incident
r	Reflected

Subscripts

0	Reference value
$1, 2, 3$	Relative to media 1, 2 and 3, resp.
p	Relative to p-polarized light
s	Relative to s-polarized light

Variables

β	Decay length $[m]$
δ	Change in phase
λ	Wavelength $[m]$
μ	Dynamic viscosity $[kg/m/s]$
ϕ	Angle relative to the normal vector of the surface
ρ	Density $[kg/m^3]$
d	Gap thickness $[m]$
D_L, D_S	Major and minor ellipse axes, resp. $[m]$
E	Amplitude of the electric field $[V/m]$
I	Light intensity $[W/m^2]$
l	Length $[m]$
n	Refraction index
r	Total reflected amplitude
r_{ij}	Reflected amplitude between media i and j

Contents

1 Introduction

Frustrated Total Internal Reflection (FTIR) is a powerful experimental technique that allows the imaging of thin films, which are important to visualise and characterise as they play a crucial role in numerous domains, be it lubrication, wetting or any other application. It was developed by Kolinski et al. [3] and is exempt from limitations of interferometry such as scale restrictions - for instance the latter technique cannot measure films thinner than the wavelength of the light source [1]. The use of a light beam to illuminate a transparent interface at an angle greater than the critical angle allows an evanescent wave to emerge in the thin film. The decay of the wave's intensity is proportional to the wavelength of the wall and is related to the distance from the interface, which allows the distance between the wall and the other medium to be known by measuring the intensity field, therefore characterizing the gap's thickness.

In this project, the final goal is to come up with a proper calibration that allows the measurement of the thin gap of air that remains trapped between a liquid drop and a solid surface for a very short amount of time before total wetting occurs, as well as to evaluate the influence of the light source's polarization in the measurements, as the reflection intensity will differ.

As a means of calibration, the small elastic deformation of a spherical lens due to its own weight on the transparent interface's surface is measured thanks to the reflected light and can be compared to the analytical solution of the deformation proposed by Hertzian theory.

2 Experimental setup

2.1 Description of the setup

This experiment follows a similar setup to the one also used by Shirota et al. [1] and is based on the same assumptions using the same equations, and is as indicated in Figure 1.

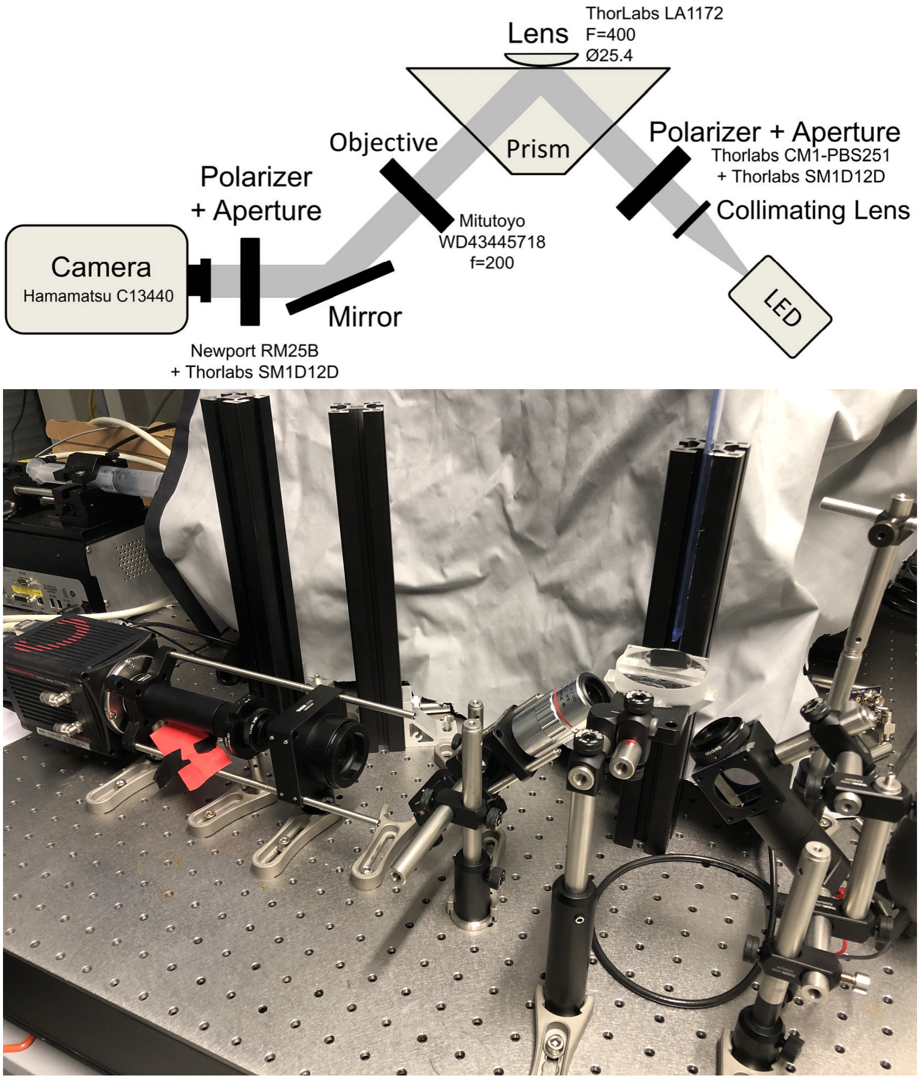

Figure 1: FTIR calibration setup with the lens

The specifications of the main components of the setup are given in Table 1. Two polarizers were placed in the setup to increase the likelihood that the light being received by the camera is polarized as intended, and apertures were added to reduce scattering as much as possible.

The light source is placed so that it at a 45^o angle compared to the ground, such that it enters the prism with a 0^o incidence angle to maximize transmittance into the prism. Index 1 refers to the medium before the light crosses the transparent interface, and is therefore the prism. Given that the prism is BK7 glass, we have $n_1 = n_{BK7} = 1.5156$ (measured experimentally) and $\phi_1 = 45°$, the latter being the angle of incidence on the transparent interface, i.e. the top surface of the prism. Index 2 refers to the medium

Component	Specifications
LED	Monochromatic green light ($\lambda = 540nm$), $20mA$ current
Lens	BK7 Glass, mass $m = 2.9186g$
Prism	BK7 Glass, isoceles right triangle
Camera	2048x2048 pixels, with link board to increase performance

Table 1: Specifications of the main components of the setup

whose thickness is being investigated, and therefore is air, $n_2 = n_{air} = 1$ and $\phi_2 = \sin^{-1}(n_1/n_2 \cdot \sin\phi_1)$ according to the Snell-Descartes law of refraction. Finally, index 3 represents the medium into which the evanescent waves are finally transmitted, which in the case of this project is the glass lens on top of the prism, also made of BK7 glass. Therefore, $n_3 = n_{BK7} = 1.5156$ and $\phi_3 = \sin^{-1}(n_2/n_3 \cdot \sin\phi_2)$.

The image read by the camera is distorted such that a circular image becomes elliptical and its aspect ratio is given by:

$$\frac{D_S}{D_L} = \frac{\cos\phi_1}{\cos(\phi_1 - 45)} \cdot \cos\left(\sin^{-1}\left(\frac{n_2}{n_1}\sin(\phi_1 - 45)\right)\right) \tag{1}$$

Where D_S is the minor axis of the ellipse or the shortened length, and D_L is the major axis or the original length. Therefore the vertical direction of the received image needs to be transformed during post processing to restore the image's correct dimensions.

Total internal reflection occurs when ϕ_1 is greater than the critical angle, given by $\phi_{c12} = \sin^{-1}(n_2/n_1)$, concerning the interface between media 1 and 2, and this is the desired condition. However, the setup must also be such that the light can propagate from medium 1 to medium 3, i.e. $\phi_1 < \phi_{c13} = \sin^{-1}(n_3/n_1)$. From Table 2 it can be found that the condition on ϕ_1 is:

$$\phi_{c12} = 41.28^o < \phi_1 < \phi_{c13} = 90^o \tag{2}$$

2.2 Gap thickness measurement

As explained previously, the air gap's height measurement is given by the distance d between media 1 and 3, or the thickness of medium 2 separating them. The change in phase of the light due to the difference in optical path by entering medium 2 and reentering medium 1 after reflection is proportional to the gap height d and inversely proportional to the decay length β:

$$\delta = \frac{jd}{\beta} = \frac{4\pi d}{\lambda}\sqrt{n_2^2 - n_1^2 \sin^2\phi_1} \tag{3}$$

Input	Value
n_1	$n_{BK7} = 1.5156$
n_2	$n_{air} = 1$
n_3	$n_{BK7} = 1.5156$
λ	$540nm$
ϕ_1	$45°$
m	$2.9186g$

Table 2: Summary of the inputs

Where j is the unit imaginary number. The total reflected amplitude is given by the ratio of the reflected amplitude and the incident amplitude:

$$r = \frac{E^r}{E^i} = \frac{r_{12} + r_{23}e^{j\delta}}{1 + r_{12}r_{23}e^{j\delta}} \tag{4}$$

The total reflected amplitude can be expressed in function of the known parameters thanks to the Fresnel equations for polarized light:

$$r_{12,p} = \frac{n_2 \cos\phi_1 - n_1 \cos\phi_2}{n_2 \cos\phi_1 + n_1 \cos\phi_2}; \qquad r_{12,s} = \frac{n_1 \cos\phi_1 - n_2 \cos\phi_2}{n_1 \cos\phi_1 + n_2 \cos\phi_2} \tag{5}$$

$$r_{32,p} = \frac{n_2 \cos\phi_3 - n_3 \cos\phi_2}{n_2 \cos\phi_3 + n_3 \cos\phi_2}; \qquad r_{32,s} = \frac{n_3 \cos\phi_3 - n_2 \cos\phi_2}{n_3 \cos\phi_3 + n_2 \cos\phi_2} \tag{6}$$

As the light's intensity is proportional to the square of the electric field,

$$I \propto |E^2| \tag{7}$$

It can be deduced that the normalized intensity is the modulus of the square of the total reflected amplitude given in equation 4:

$$I_{normalized}(x,y) = |r^2(x,y)| \tag{8}$$

This gives a unique relation between $I_{normalized}$ and d regardless of whether ϕ_1 is greater or smaller than the critical angle, and therefore means that measuring $I(x,y)$ and a reference $I_0(x,y)$ will quantitatively measure d. The relationship between the gap d and the normalized intensity $|r^2|$ is plotted in Figure 2 for $s-$ and $p-$polarized light, along with the curve for the relation assuming total energy transfer (and neglecting the role of polarization) used by Kolinski et al. in previous works [3, 2, 5]:

$$d = -\delta \log\left(1 - \frac{I(x,y)}{I_0(x,y)}\right) \tag{9}$$

Notable is the fact that for a same gap height, the normalized reflection intensity is higher for s-polarized light than it is for p-polarized light.

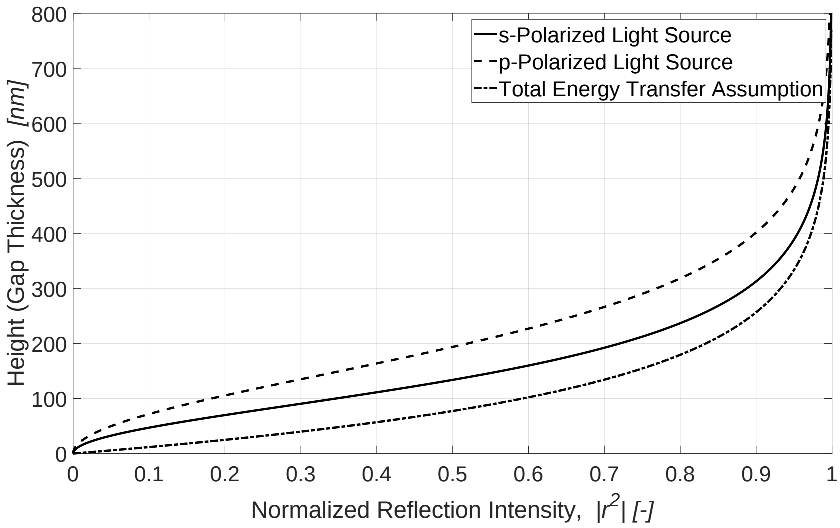

Figure 2: Mapping between the gap thickness and the normalized reflection intensity for BK7 glass with an incident angle of 45°. Note that the slope is less steep for $s-$polarized light

2.3 Validation with the Hertzian model

The measured radial profile of the lens is compared afterwards to the analytical solution proposed by Hertzian theory of solid contact, as it is laid out by Shirota et al. [1] There should therefore be a non-zero circular contact area between the prism and the deformed lens.

3 Calibration results

3.1 Reference images

After the setup has been put in place properly, the first important step to take is to capture reference images for both $s-$ and $p-$polarized images, i.e. record images of the top of the prism without the lens. To overcome the error caused by the noise of the data contained in a single image, 30 images were taken consecutively every $1500ms$ over time and the final reference image is made using the time-average of the data of the 30 images. The exposure time of the camera was set to $600ms$ for both $s-$ and $p-$polarized images to take advantage of as much of the camera's bit depth as possible. The images would then yield a 2048x2048 discrete reference intensity function, $I_0(x, y)$, for both $s-$ and $p-$polarized light.

The software that reads the camera's image is Micro-Manager 1.4, and the post processing of the data is done in MATLAB. Some reference images can be seen in Figure 3.

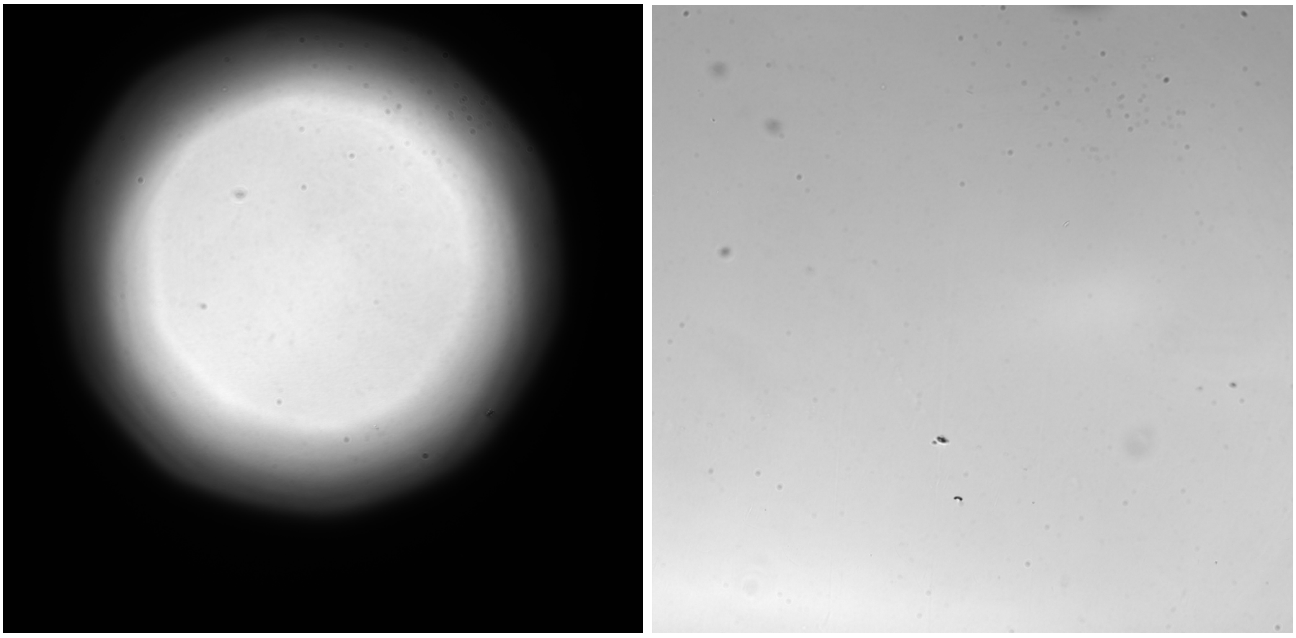

(a) $s-$polarized with apertures present (b) $p-$polarized without apertures

Figure 3: Reference images taken with the Hmamatsu C13440 camera

Initially, the normalization was done by dividing the measured intensity by the reference intensity. However, due to error caused by ambient noise and other perturbations, a new normalization method was used: for this the square root of the intensity was considered as the reflected electric field's amplitude is related to the intensity's square root:

$$I_{normalized} = \left(\frac{\sqrt{I} - \sqrt{I_{noise}}}{\sqrt{I_0} - \sqrt{I_{noise}}} \right)^2 \quad (10)$$

The subtracted I_{noise} term is the measured intensity with the light source switched off, considered as a perturbation offset.

This normalization gives an error compared to the Hertz solution that is quite small and does not suffer from a large offset around the center of the lens like the results presented by Shirota et al. [1]

The mapping of spatial position given in pixel indices to spatial coordinates in millimeters was found by placing a ruler in lieu of the prism, showing that the 2048 pixel length measures around $3.2mm$ for the used setup (cf. Figure 4).

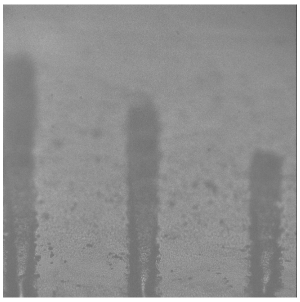

Figure 4: Ruler showing the scale

3.2 Captured images

Looking at the transfer functions plotted in Figure 2, one notices that the slope is less steep for $s-$polarized light making the inversion easier to perform as sensitivity to noise is less pronounced. Also, given that the quality of the $s-$polarized images was superior in terms of clarity of the lens's profile and noise, it was chosen to concentrate only on *$s-$polarized images from here on.* Figures 6 and 7 show the good results obtained from the current setup as the error is quite small - most measured values have less than $15nm$ of error!

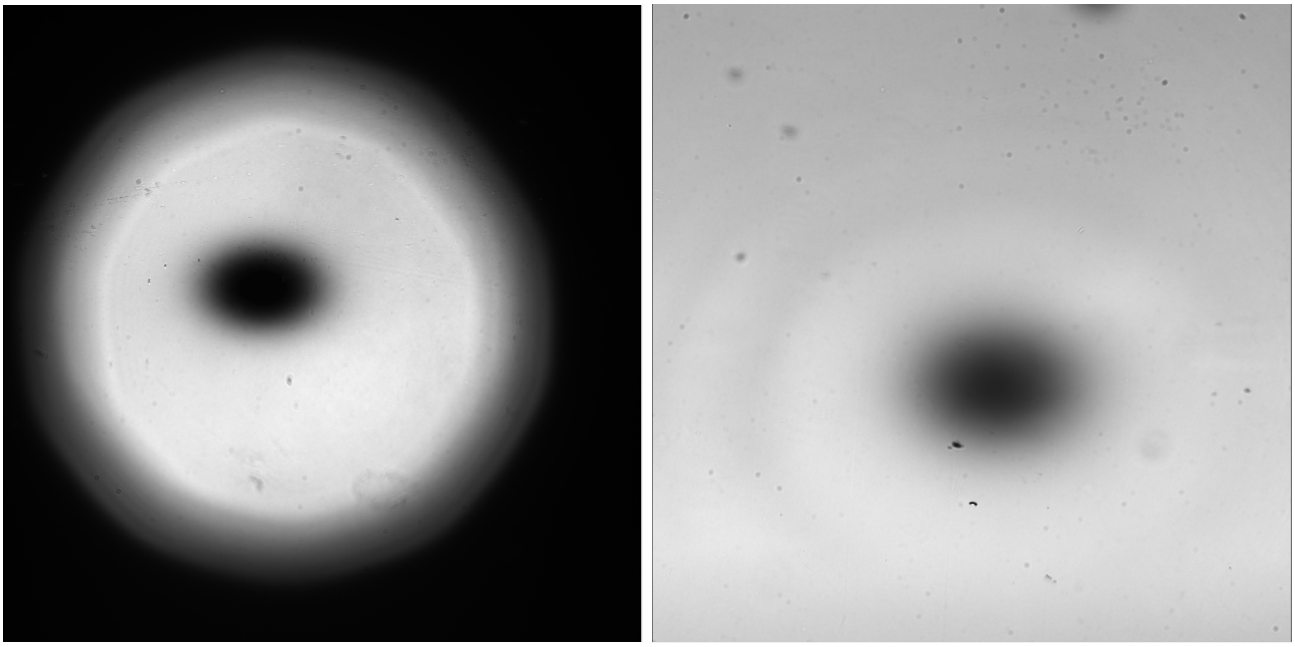

(a) $s-$polarized (b) $p-$polarized

Figure 5: Captured images with the lens above the prism. Note that the $p-$polarized image shows the lens less clearly than the $s-$polarized image.

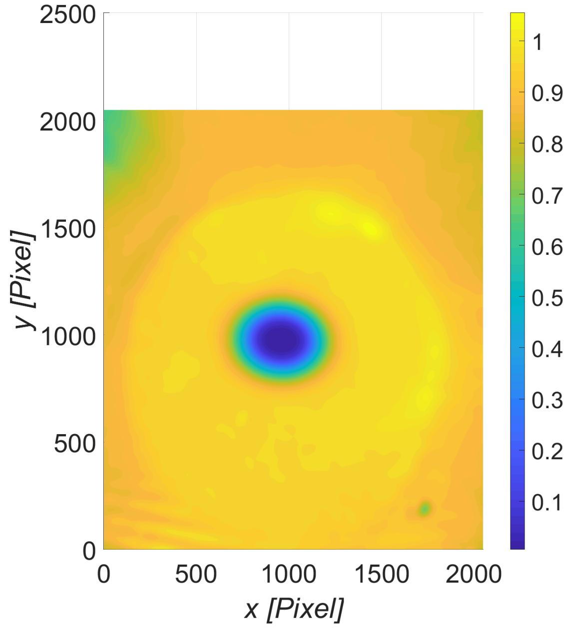

Figure 6: Normalized intensity with the lens on top of the prism. The sudden drop in intensity far from the lens is due to the aperture's restriction.

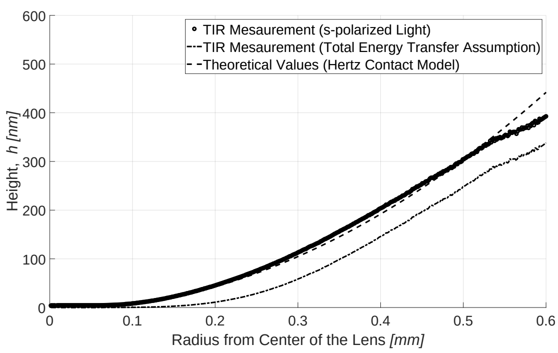

(a) Gap measurement, or lens profile measurement

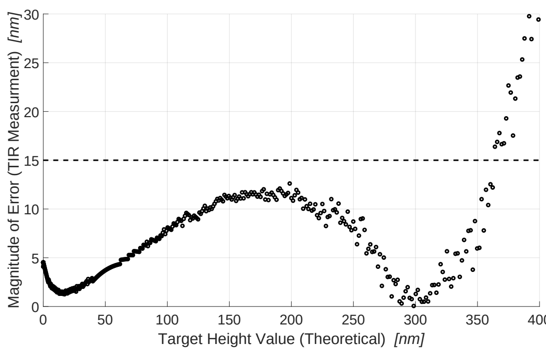

(b) Error between the $s-$polarized measurement and the Hertzian solution

Figure 7: Comparison of the measured lens profile or air gap with the theoretical Hertzian curve and compared to the previous work done assuming total energy transfer by Kolinski et al. [3, 2, 5], and the error between the new measurement and the Hertzian model

3.3 Mica sheets

The use of very thin mica sheets on the top surface of the prism, as done previously by Kolinski [4], was attempted at the end of the calibration process. The reasoning is that the sheets' thickness are of atomic scale and extremely smooth, making the experimental setup optimal for droplet impacts and the visualization of the thin air layer between the solid and liquid easier. The mica sheets were linked to the top of the prism with immersion oil.

Unfortunately, the image obtained was consistently of questionable quality as the image was double and slightly offset, and a satisfactory solution to this problem could not be found in time. Whether this is linked to its higher refractive index of around 1.56 to 1.61 is to be determined [6]. Therefore it was chosen to proceed by omitting the mica sheets and keeping the top of the prism bare.

4 Droplet impacts

One droplet impact experiment was performed using isopropanol drops, from a very low height. The captured image revealed that a continuous light source isn't an appropriate match for the camera at very high framerates as a peculiar and unexpected line and deformation across the middle of the drop can be seen (cf. Figure 8) - this is due to the way the image acquisition's algorithm reconstructs the picture and the problem can be overcome by pulsing the light source at a frequency that is synchronized to the camera's exposure time.

However, in Figure 8 the thin layer of air is clearly distinguishable and present. The frame acquisition rate needs to be increased compared to this experiment (around 100 fps), however, because the trapped air is only visible for around 2 frames, and the light source's intensity needs to be increased to counteract the minimized exposure time.

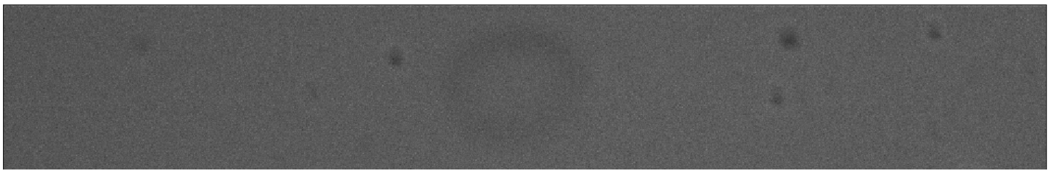

(a) $t = t_0$ as the drop reaches the prism

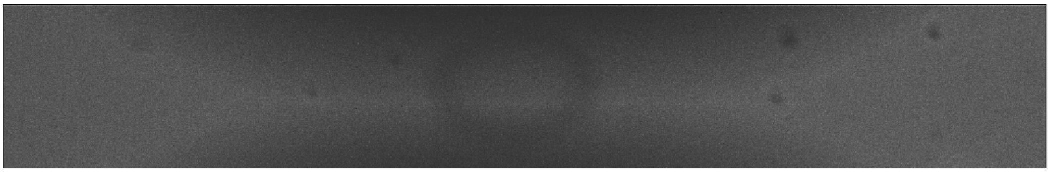

(b) $t = t_0 + 10ms$

Figure 8: Isopropanol droplet impacting from a few millimeters height on top of the prism with the trapped air layer clearly visible. The unexpected line and deformation in the middle are due to the reconstruction of the picture

During the final days of this project a circuit board was being assembled to introduce a higher intensity, pulsing LED into the setup, however this was not finished in time to be used in the experiment.

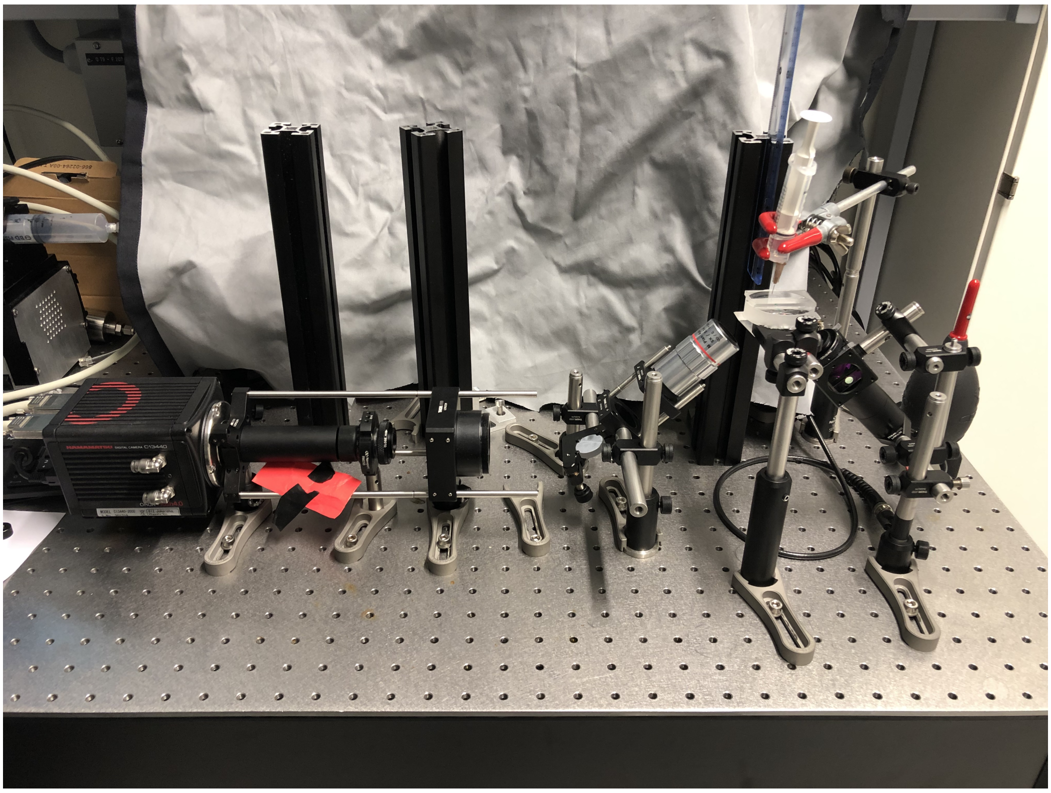

Figure 9: Experimental setup ready for isopropanol droplet impacts

5 Conclusion

Once the setup was put in place, post processing posed a rather substantial challenge as to how the captured images could be used to measure the lens' profile as accurately as possible. The new proposed normalization method eliminates most of the perturbation caused by ambient noise and therefore excludes one of the biggest sources of error in the measurement, and doesn't contain a considerable error around the middle of the lens like Shirota et al. do in their measurements [1].

A big question that remains is precisely why there is such a noticeable difference in the quality of the $s-$polarized images versus the $p-$polarized ones. It is of course known that the reflectance of both kinds of light are different in identical media under the same incidence, but this does not shed much light on why the error and amount of noise is consistently greater in one than in the other.

More further work to be done would be the proper addition of mica sheets to the setup without their presence negatively affecting the quality of the measurements. Then, the next big step would be to properly implement a pulsing LED with a higher intensity that is synchronized with the camera to try and overcome the deformations in the measured images caused by the reconstruction.

The implementation of these proposed steps would finally allow droplet measurements to be performed from different heights to validate the fitness of this calibration to droplet impact measurements.

References

[1] Minori Shirota et al. “Measuring thin films using quantitative frustrated total internal reflection (FTIR).” In: *The European Physical Journal E 40.5* (2017).

[2] John M Kolinski, L Mahadevan, and Shmuel M Rubinstein. “Lift-off instability during the impact of a drop on a solid surface.” In: *Phys. Rev. Lett.* 112.13 (2014), p. 134501.

[3] John M Kolinski et al. “Skating on a film of air: drops impacting on a surface.” In: *Phys. Rev. Lett.* 108.7 (2012), p. 074503.

[4] John Martin Kolinski. “The role of air in droplet impact on a smooth, solid surface.” PhD thesis. 2014.

[5] John Martin Kolinski, L Mahadevan, and SM Rubinstein. “Drops can bounce from perfectly hydrophilic surfaces.” In: *Europhys. Lett.* 108.2 (2014), p. 24001.

[6] *Mica Sheets and Disks.* `https://www.emsdiasum.com/microscopy/products/preparation/mica.aspx`. last consulted on Jan. 10, 2018.